High Power, *p-i-n* Diode Controlled, Microwave Transmission Phase Shifters

J. F. WHITE, MEMBER, IEEE

Abstract—An iterative circuit, diode, transmission phase shifter is discussed, having a canonic form that consists of a length of transmission line symmetrically loaded at its ends by small susceptances whose values are diode controllable. The spacing of the susceptances is chosen so that their reflections are nearly mutually cancelling, (about a quarter wavelength if equal magnitude, opposite sign susceptances are used). A change of electrical length of the section of 23°, in principle, is obtainable with a maximum input VSWR of 1.04. Eight section, experimental circuits yielded 180° total phase shift with less than one decibel of loss in the *L* and *S* bands and peak RF power capability to 15 kilowatts. Operation to 140 kilowatts peak power was achieved with reduced phase shift per section. The transmission phase shifter is believed to be well suited as a phase control element for beam steering of array antennas.

I. Introduction

MANY RADAR DESIGNS currently proposed, incorporate phased array antennas. This form of microwave radiator is advantageous in that its pattern can be steered, even subdivided into multibeams, at high speed. Its power is not limited by the finite capacity of its subradiators, only by their number. Numerous methods have been recommended to control the phase of the coherently energized subradiators in order to direct the antenna pattern that results from their aggregate radiation. The use of two-port controllable time delay circuits in series with each element, indicated schematically in Fig. 1, is conceptually a straightforward solution.

In principle, by this method, the same antenna pointing direction is achieved simultaneously for any radiating frequency, $f=\omega/2\pi$. This feature is very desirable. Not only does it permit simultaneous, variable frequency operation, but it is nonrestrictive of the RF amplitude modulating envelope that can be exploited effectively in the radar's operation. However, design of a satisfactory multiwavelength time delay circuit often is difficult. Particularly, insertion loss and phase dispersion effects may so compromise its performance that a phase shifter, which is more easily implemented, is judged a more practical control element. It can effect the same steady state beam steering at a single frequency that is provided by the switchable delay line. For example, control of the radiation phase, ϕ, in the circuit of Fig. 1 could be employed, recognizing that $\sin(\omega\tau_n)=\sin(2k\pi+\phi)$ where k is integer and sufficiently large that $0\leq\phi<2\pi$.

Manuscript received September 4, 1964; revised December 21, 1964. This work was sponsored, in part, by the Navy Bureau of Ships under Contracts NObsr-81470 and NObsr-87291.

The author is with Microwave Associates, Inc., Burlington, Mass.

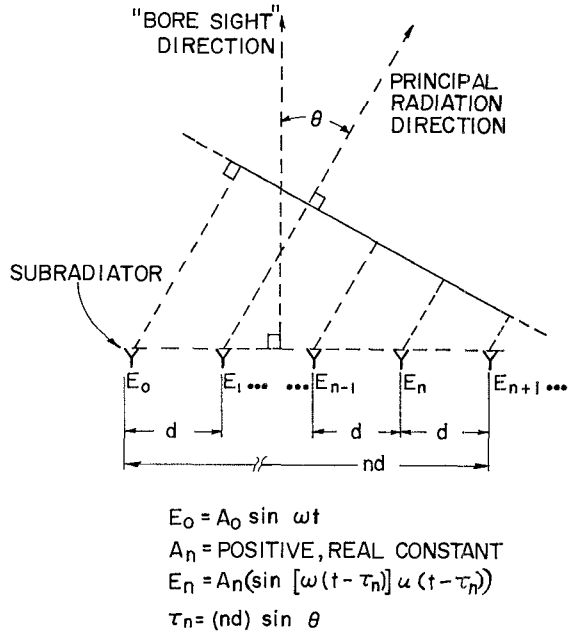

Fig. 1. Schematic diagram of a linear array antenna pointed at an angle θ off boresight by time delay circuits.

For most applications, the ideal form of phase shifter circuit is a two-port network having a transfer function of unit amplitude and electronically variable phase. A typical circuit, the transmission-reflection type, consisting of a circulator with a diode controllable reflective phase termination is shown in Fig. 2(a). In fact, this method achieves controllable time delay of arbitrary length if the diode is assumed to switch between short and open circuit impedances. Bilateral performance at twice the power level can be achieved with the similar, hybrid coupler version shown in Fig. 2(b) [1]-[4]. Symmetry of the terminations in the latter case is necessary to maintain a match at the coupler's input port.

Diodes have a maximum tolerable power level capacity commensurate with the phase shift they provide [5]. Necessarily, the phase shift obtained per diode is made to be small for high power operation, and this suggests the use of networks designed about small perturbation techniques. An acceptable transmission match can be obtained without a circulator of hybrid coupler under these circumstances. This is exemplified by the ideal canonic circuit of Fig. 3(a), wherein a symmetric pair of variable susceptances perturb the phase of the transmission coefficient of the intervening line section. Their spacing is selected to make reflections practically mutu-

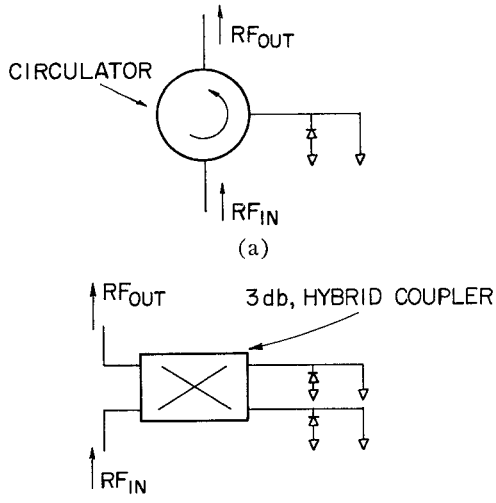

Fig. 2. Transmission-reflection time delay circuits.

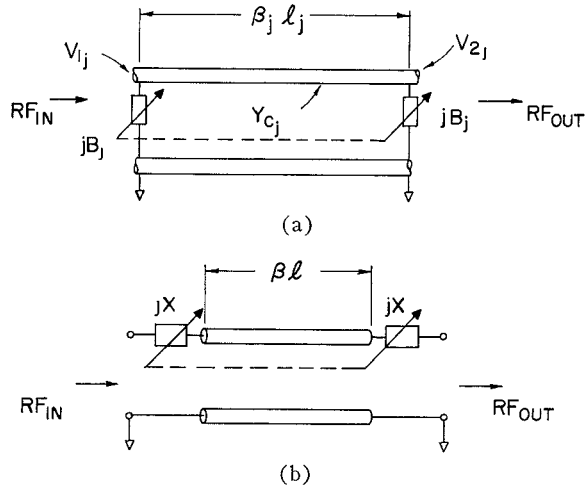

Fig. 3. Ideal, lossless transmission type phase shifter prototype sections.

ally cancel over the small, susceptance-variation control range. This transmission type phase shifter is to be discussed. Other similar circuits[1] are useable, such as the Dual Circuit shown in Fig. 3(b). Theoretically, it is capable of the same performance, but it is usually less desirable in practice because its biasing circuit requires more isolating elements.

II. Analysis

A. Exact Solution

The phase shift $\Delta\phi$ of an n section cascade is defined in Fig. 4(a). A small amount of phase shift is obtained from canonic sections of the form shown in Fig. 4(b). Several sections can be cascaded, Fig. 4(c), to provide multistep phase control; usually a range of up to 2π radians is desired. The phase shift contribution of any particular section is influenced by the input and output load admittances referred to its terminals by the circuit to which the section is connected. Therefore, the total phase shift of the cascade, $\Delta\phi$, is not necessarily equal to the sum of the individual values, $\Delta\phi_j$, which would be measured for each section when it is mounted between matched source and load admittances. However, this sum,

$$\sum_{j=1}^{n} \Delta\phi_j$$

approaches the value $\Delta\phi$ if all sections are designed for low VSWR. It is therefore a useful design approximation and will be discussed subsequently.

Since the transmission properties of the general canonic network of Fig. 4(b) are of predominant interest, the $ABCD$ matrix provides a convenient analysis representation. Phase shift and loss are defined relative to the voltage V_0 of the Thevenin generator; since the input voltage V_1 to the network does not remain constant with the perturbation of the twoport's parameters, A, B, C, and D except in the special cases in which the perturbation leaves unchanged the ratio of the driving (generator) impedance to the input impedance of the cascade. That is to say, the output voltage of the generator changes with its loading.

The phase shift, $\Delta\phi$, of the two-port network is defined as the change in transfer phase, ϕ, which results when the A, B, C, D parameters of the complete network are perturbed. This occurs in the present discussion because the admittance values of each section are assumed to be variable. In general, consider that losses of the transmission line and the control admittances are significant, and that the line characteristic admittance Y_C may be complex. Furthermore, assume that in the n section cascade of Fig. 4(c), each section can be unique with respect to Y, Y_C, and γl. Then an exact solution to the cascade's parameters is obtainable from the matrix product of Fig. 4(c).

In the high power, diode phase shifters to be described, the admittance values are controlled in discrete increments by means of *p-i-n*, two state, switching diodes. This analysis applies equally well, however, for continuous admittance variation as could be effected with line shunting elements incorporating varactor diodes. In any case, a practical phase shifter is to be represented by the cascade shown in Fig. 4(c). Its characterization consists in ascertaining the total insertion loss and transfer phase for particular combinations of section admittance values. In some applications, input VSWR may be of interest also.

Hand calculations of the phase shift, insertion loss and input VSWR, even for a single prototype section, by the exact method are laborious, and computer solution of this matrix relation is desirable. Approximate expressions for phase shift and insertion loss of sections along with means for estimating the maximum input

[1] A three element transmission phase shifter for use at low RF power levels is discussed by Dawirs, H. N., and W. G. Swarner, A very fast, voltage-controlled microwave phase shifter, *Microwave J.*, Jun 1962, pp 99-106.

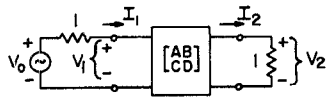

$$V_1 = AV_2 + BI_2$$

$$I_1 = CV_2 + DI_2$$

$$V_0/V_2 = (A+B+C+D)$$

(a)

TRANSFER PHASE = ϕ = ARG $\left[V_0/V_2\right]$

PHASE SHIFT = $\Delta\phi$ = ARG $\{V_0/(V_2+\Delta V_2)\} - \phi$

INSERTION LOSS = IL. = $\left|V_0/2V_2\right|^2$

INPUT REFLECTION COEFFICIENT = $\rho e^{j\delta} = \frac{A+B-C-D}{A+B+C+D}$

INPUT VSWR = $\frac{1+\rho}{1-\rho}$

(b)

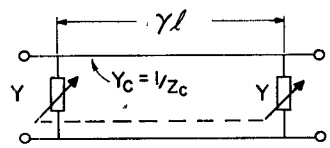

$Y = G + jB$

$\gamma = \alpha + j\beta$

(c)

$$\begin{bmatrix} A & B \\ C & D \end{bmatrix}_{XY} = \prod_{k=1}^{n} \begin{bmatrix} \cosh(\gamma\ell)_k + (Z_C Y)_k \sinh(\gamma\ell)_k & Z_{C_k} \sinh(\gamma\ell)_k \\ \left\{ \begin{matrix} Y_k \cosh(\gamma\ell)_k + (Z_C Y^2)_k \sinh(\gamma\ell)_k \\ + Y_{C_k} \sinh(\gamma\ell)_k + Y_k \cosh(\gamma\ell)_k \end{matrix} \right\} & \left\{ (Z_C Y)_k \sinh(\gamma\ell)_k + \cosh(\gamma\ell)_k \right\} \end{bmatrix}$$

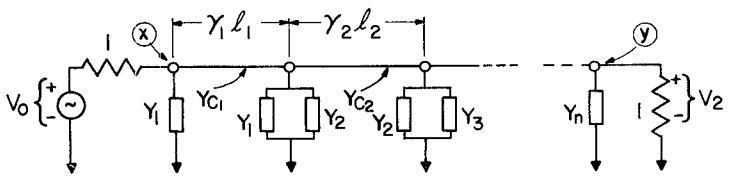

Fig. 4. Defining relationships and exact solution for an n-section transmission phase shifter cascade. (a) Definitions. (b) Canonic circuit form. (c) Cascade of n sections.

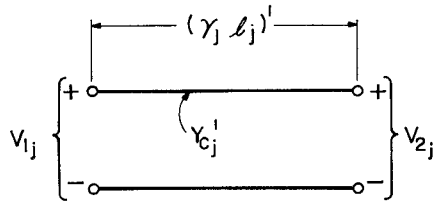

GENERAL CASE:

$$(\gamma_j \ell_j)' = \cosh^{-1}(\cosh \gamma_j \ell_j + Z_{cj} Y_j \sinh \gamma_j \ell_j)$$

$$Y_{cj}' = Y_{cj} \left[1 + (Z_{cj} Y_j)^2 + 2 Z_{cj} Y_j \coth \gamma_j \ell_j\right]^{1/2}$$

LOSSLESS CASE:

$$(\beta_j \ell_j)' = \cos^{-1}(\cos \beta_j \ell_j - B_j Y_{cj} \sin \beta_j \ell_j)$$

$$Y_{c_j}' = Y_{cj}\left[1 - (Z_{cj} B_j)^2 + 2 Z_{cj} B_j \cot \beta_j \ell_j\right]^{1/2}$$

Fig. 5. Uniform transmission line equivalent of the jth section of the phase shifter cascade.

VSWR of their cascade combination will now be discussed. The approximate methods are especially useful for design purposes because, in addition to computational simplification, they lend insight into the quantitative effects to be obtained from particular circuit parameter variations. A typical procedure is to design individual sections using the approximate expressions for phase shift and insertion loss of a section, and then make the further approximation that they will yield the same phase shift and insertion loss contributions when cascade mounted to form a multisection phase shifter. The resulting design then can be evaluated either by the exact solution method or by construction of an experimental model. Both of these verification means are desirable in the design refinement of a phase shifter for which construction in the large quantities typically required for a phased array is intended.

B. Approximate Solution

1) *Uniform Line Equivalent Circuit:* In Fig. 5 is shown the relationship between the jth, loaded-line, phase shifter section of Fig. 4(c) and an equivalent unloaded uniform line length. In general, the actual transmission line Y_{Cj} and its unloaded equivalent Y_{Cj}' can have complex characteristic admittances. In the approximate analysis, however, it will be assumed that Y_{Cj} is a scalar, normalized to unity in both magnitude and dimension.

The phase shift of this jth section will be calculated using the lossless equivalent circuit shown in Fig. 3(a). Subsequently, insertion loss will be calculated by allowing a second order, small perturbation conductance to be added to the control susceptances and a small amount of uniform loss in the intervening transmission line section. Even for the lossy approximation case, the line will be assumed distortionless, $Y_{Cj}=1$. The phase perturbation Δ Arg (V_{1j}/V_{2j}) to the line length $\beta_j l_j$ effected by the shunt loading at its ends with susceptances jB_j is approximately the difference, $(\beta_j l_j)'-\beta_j l_j$.

2) *Phase Shift of the Lossless Network:* Consider the lossless circuit of Fig. 3(a) and assume that the shunt susceptances both switch from B_{j1} to B_{j2}, and that these have + and − signs respectively. The unloaded line equivalent circuit corresponding to this network then would undergo a change of electrical length $\Delta\theta_{j(1,2)}$ given by (1) [6].

$$\Delta\theta_{j(1,2)} = \Delta\theta_{j1} + \Delta\theta_{j2}$$

$$\Delta\theta_{j(1,2)} = \cos^{-1}(\cos\beta l - B_{j1}\sin\beta l) - \cos^{-1}(\beta l - B_{j2}\sin\beta l) \quad (1)$$

Equation (1) is interpreted geometrically in Fig. 6. The j subscript, denoting the section number, is omitted in the diagram for simplicity. In this description, the unloaded line length $\beta_j l_j$ is represented as a unit magnitude vector which is rotated, or perturbed, by a susceptance pair B_{ji} in angular amounts equal to the perturbation length $(\beta_j l_j)'-\beta_j l_j$ previously described. Shown

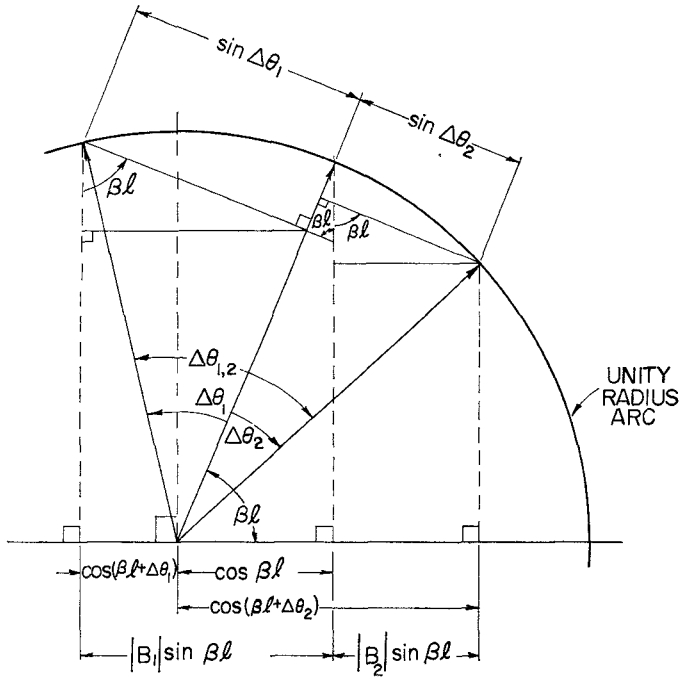

ASSUME B_1 AND B_2 HAVE (+) and (−) SIGNS RESPECTIVELY

$$\sin\Delta\theta_1 = |B_1| - (1-\cos\Delta\theta_1)\cot\beta\ell$$

$$\sin\Delta\theta_2 = |B_2| + (1-\cos\Delta\theta_2)\cot\beta\ell$$

if $\Delta\theta_1$ AND $\Delta\theta_2$ ARE SMALL AND $\beta\ell \approx 90°$

then $\Delta\theta_{1,2} \approx |B_1| + |B_2| = B_1 - B_2$

Fig. 6. Geometric derivation of an approximate solution for $\Delta\theta_i$ defined by the expression $\{\cos(\beta l+\Delta\theta_i) = \cos\beta l - B_i \sin\beta l\}$.

is a counter-clockwise rotation for a positive (lengthening) phase shift increment $\Delta\theta_{j1}$ and a clockwise rotation denoting a negative (shortening) increment $\Delta\theta_{j2}$. The vectors are constructed so that their projections on the horizontal axis satisfy the relation $\cos(\beta l+\Delta\theta_{ji}) = \cos\beta l - B_{ji}\sin\beta l$.

Associating signs with the angular perturbations, the total change in the length of the unloaded line equivalent circuit of the jth section which results when the shunt susceptance pairs of the section switch from B_{j1} to B_{j2} is $\Delta\theta_{j(1,2)}$. Now $\Delta\theta_{j(1,2)}$, the change in electrical length of the unloaded line, equivalent circuit is approximately equal to the phase shift, $\Delta\phi_j$, that would be measured for the jth section if it were mounted between unity source and load admittances. In turn,

$$\Delta\phi \approx \sum_{j=1}^{n} \Delta\phi_j.$$

Both expressions become exact, i.e.,

$$\Delta\theta_{j(1,2)} = \Delta\phi_j \quad \text{and} \quad \Delta\phi = \sum_{j=1}^{n} \Delta\phi_j$$

If $Y_{Cj}' = Y_{Cj} = 1$ for all values of j.

In Fig. 6, an approximation to (1) is derived. This result, given by (2), indicates that if βl is about 90° and if shunt perturbations are small, then the phase shift (in radians) is equal simply to the difference in normalized switched susceptances. The same conditions under which (2) is accurate also yield near reflectionless transmission for the small susceptance, line-loading elements.

$$\Delta\theta_{j(1,2)} \approx B_{j1} - B_{j2} \tag{2}$$

If the section is terminated in a unity admittance, its maximum input VSWR is bounded as shown in (3) [6]. The maximum occurs when the equivalent line length is an odd multiple of quarter wavelengths. Equation (3) applies for an arbitrarily long cascade of identical sections provided all shunt susceptances, B_{ji}, of the cascade have the same magnitudes.

$$\begin{aligned} \text{VSWR} &\leqq (Y_C')^2 \qquad \text{if } Y_C' \geq 1 \\ \text{VSWR} &\leqq (1/Y_C')^2 \qquad \text{if } Y_C' \leq 1 \end{aligned} \tag{3}$$

Actually, in practice, sections may not have the same susceptance magnitude in both bias conditions; they may be switched one, or a few at a time, in order to achieve multi-increment control of the cascade's transmission phase. Under these circumstances, the equivalent unloaded-line relative admittances Y_{Cj}' and electrical lengths $\beta_j l_j'$ of each section of the cascade can be calculated for any B_{ji} control combination; and the input VSWR determined for their series aggregate using transmission line analysis.

As a parameter-value example for a typical section, suppose that $\beta l = 90°$ and $B_{1,2} = \pm 0.2$, respectively; then a phase shift, $\Delta\theta$, of about 0.4 radians or 23° is obtained by switching the line loading values from B_1 to B_2. This value would be the phase shift obtained with matched source and load terminations. The loaded line section would have an unloaded line equivalent for which $Y_{C1}' = Y_{C2}' = 0.98$ and $(\beta l)_{1,2}' = 78\frac{1}{2}°$ and $101\frac{1}{2}°$, respectively. The maximum input VSWR of an n section unity admittance terminated cascade of such circuits could not exceed 1.04. Therefore, the resulting phase control expected for the cascade would be $\Delta\phi \approx p \cdot 23°$, $(p = 0, 1, 2, \cdots, n)$.

3) *Calculation of Insertion Loss:* Three causes exist whereby the ratio of power delivered to the load by the cascade to that available from the generator is diminished. First, reflections can exist at the inputs and outputs to the sections, causing mismatch interaction. Such reflections influence both phase shift and insertion loss, but they are typically negligible with proper design. The remaining two loss mechanisms are those due to the real part α of the transmission line propagation constant $\gamma = \alpha + j\beta$ and from the conductive portion G_j of the controlled admittances $Y_j = G_j + jB_j$.

Line losses are treated as if they were the same as they would be with the shunt admittances removed. The fractional loss of incident power in each Y_j is equal approximately to the numerical value of its normalized conductance G_j. These approximations, also, imply that the perturbations Y_j are small and that the prototype sections are nearly matched.

As an example, consider the sample case previously described. If the shunt susceptances are replaced by values $Y_{1,2}$ equal to $0.02 + j0.20$, and $0.02 - j0.20$, respectively, and if the transmission line has a loss of 0.1 decibel per wavelength, then a total loss of 0.19 dB would be estimated for the section.

4) *Estimated Accuracy of the Approximate Solutions:* The exact expression for transfer characteristic given in Fig. 4 reduces to the form of (4) for the doubly match-terminated, single section case.

$$\begin{aligned} \frac{V_0}{V_2} &= (2 + 2Y)\cosh(\gamma l) \\ &\quad + (Y_C + Z_C + 2Z_C Y + Z_C Y^2)\sinh(\gamma l) \end{aligned} \tag{4}$$

Solving this expression under the conditions of the previous example with $Y = 0.02 - j0.20$, but βl even as small as 80°, exact values for phase shift and insertion loss are 11.29° and 0.195 dB. These compare well with 11.46° and 0.186 dB calculated for the same conditions using the approximate method. Thus, the approximate method probably can be expected to be accurate within a few per cent over a ± 10 per cent bandwidth when applied to a doubly match-terminated, single section with circuit perturbation values no larger than those described. However, in practice, admittance variations with frequency must be considered. Also, estimation of the performance of a cascade of several sections using the approximate solution can produce cumulative errors. Nevertheless, this method is useful for initial design purposes, as implied by the following experimental results.

III. Experimental Verification

A. L-Band Model

1) *Diode Equivalent Circuit:* At L-band frequencies, high-voltage p-i-n switching diodes have impedances that vary essentially from a short circuit at forward bias (+100 milliamperes) to an open circuit at reverse bias (−100 volts) when referred to a 50 ohm transmission line impedance. Accurate microwave measurements of the diodes' equivalent circuit parameter values are difficult to make for this reason. Certain of the values have been reported by Stark [4] for diodes of this type. A compilation of typical data is given in Fig. 7 that was assumed to apply for the diodes used in the L- and S-band models. The reader is referred to Stark [4], Leenov [7], and DeLoach [8] for discussions of diode impedances.

2) *Controllable Susceptance Implementation:* In Fig. 8 is shown the equivalent circuit and approximate phase shift relation for a particular implementation of the transmission phase shifter suitable at L-band frequencies. In order to maintain the least perturbation to the

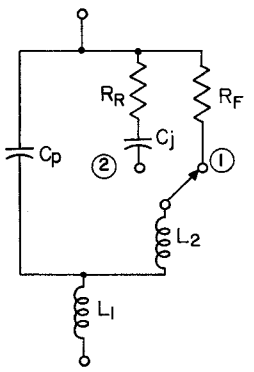

① FORWARD BIAS (+100 MA)

② REVERSE BIAS (-100 VOLTS)

EQUIVALENT CIRCUIT:

PIN DIODE IN MICROWAVE ASSOCIATES' PILL III OR PILL IV PACKAGES

TYPICAL PARAMETERS

PARAMETER	VALUE		REMARK
R_F	0.4 to 0.8	Ω	-MEASURED AT 600 Mc and 3kMc
R_R	0.8 to 1.2	Ω	-MEASURED AT 3 kMc and -90V. REPORTED RESULT[REF.4]
C_p+C_j	0.7 to 1.0	PF	-MEASURED AT 1Mc and -50V
C_p	0.2 to 0.4	PF	-EMPTY PACKAGE MEASUREMENT
L_1+L_2	0.8	nH	-ESTIMATED, INDUCTANCE IS A FUNCTION OF MOUNTING AS WELL AS PACKAGE

Fig. 7. *p-i-n* switching diode equivalent circuit.

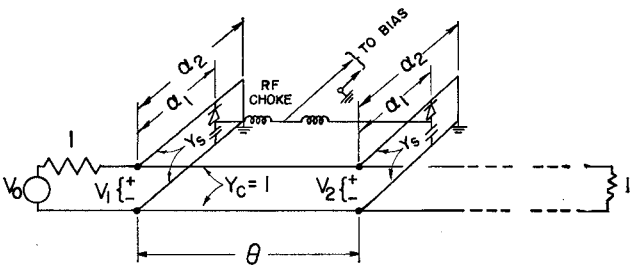

IF $(\alpha_2+\alpha_1)/2 \approx 90°$

AND $\theta \approx 90°$

AND $\alpha_2-\alpha_1$ = SMALL ANGLE

THEN, $\Delta\phi = \Delta \text{ ARG}(V_2/V_0) \approx Y_s(\alpha_2-\alpha_1)$

Fig. 8. Equivalent circuit of switchable stub phase shifter for use at L band.

transmission line and achieve a maximum phase shift per section, it is desirable that the shunt susceptance values $B_{1,2}$ be equal in magnitude and opposite in sign. This is effected quite easily with the circuit shown by switching the length of a short-circuited transmission line stub about an average value of 90° using a *p-i-n* diode. Then, the resulting change in susceptance shunting the main transmission line is approximately equal to $Y_s(\alpha_2-\alpha_1)$. The phase shift, in turn, is approximately equal to $(Y_s/Y_C)(\alpha_2-\alpha_1)$. The RF voltage impressed across the diode under reverse bias is approximately proportional to sin $(\alpha_2-\alpha_1)$. Very high power operation requires that this be small. Moreover, for a particular $(\alpha_2-\alpha_1)$ phase shift increases with Y_s/Y_C, and with

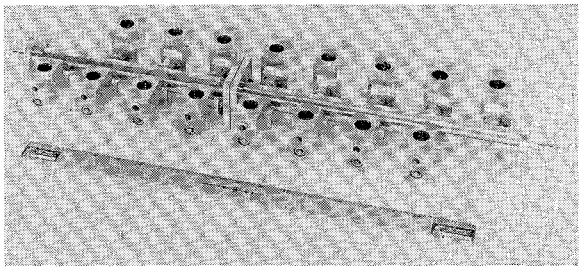

Fig. 9. Photograph of eight-section (16-diode) L-band transmission phase shifter model.

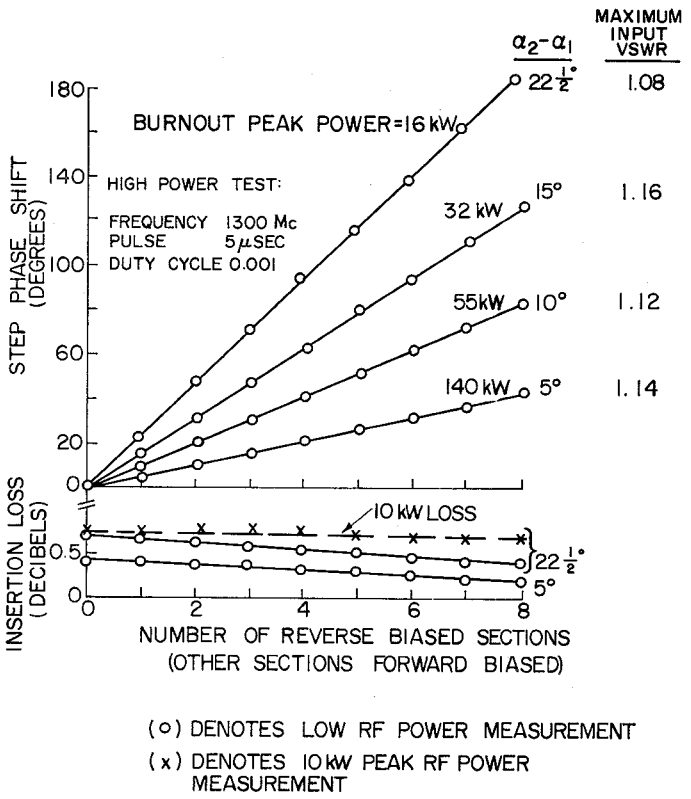

Fig. 10. L-band measurements of phase shift, insertion loss and ultimate peak power capability.

it the RF current that the diode must sustain under forward bias is also increased.

3) *Measured Results:* An eight-section experimental model was constructed as shown pictorially in Fig. 9. The values α_1 and α_2 were made adjustable about a center value which would yield about $22\frac{1}{2}°$ of phase shift at 1300 Mc/s. The diode in each stub was mounted in series with a bypass capacitor, as shown in Fig. 8, of about 25 pF. This served as a bias isolation connection as well as an approximate series resonator of the diode and mount inductance L_1+L_2. Thusly, the stub was short circuited near the diode position when the diode was forward biased. Characteristic impedance levels of 50 ohms were used both in the main transmission line and the stubs. Measurements made at low RF power, a few milliwatts, of phase shift and insertion loss are plotted in Fig. 10. No change in phase shift was observed under the high power excitation described in Fig. 10, but some increase of insertion loss did occur

under the reverse bias condition of the diodes, as indicated in the data. Similar nonlinear loss effects have been noted for *p-i-n* diodes by Temme [3], and Stark and Burns, et al. [4].

For each value of $\alpha_2-\alpha_1$ that was investigated, the average stub length was made approximately equal to 90° and all stubs were adjusted mechanically to the same dimensions. As may be seen from the measured data, a relatively close experimental reproducibility of the phase shift from section to section was obtained without electrical fine tuning. The incremental phase shift per section varied between 21° and 24°; the average value was 23° for a total of 184° phase shift with the eight-section cascade at the center frequency, 1300 Mc/s. Phase shift was measured at the input and output terminals of the cascade using an RF bridge with a calibrated trombone line.

The total, low RF power level, insertion loss, shown in Fig. 10, had a maximum value of 0.7 dB when all diodes were forward biased and a minimum of 0.35 dB with all reverse biased. Circuit losses with diodes removed were 0.3 dB. Diode loss values of 0.3 dB (forward bias) and less than 0.1 dB (reverse bias) would be estimated from the assumed circuit values shown in Fig. 7; thus, the measured loss values are of the order expected. An equalization of the forward and reverse loss values could be achieved by using a higher stub characteristic impedance. This would reduce the voltage limited peak power handling capability because a larger increment of switched stub length $\alpha_2-\alpha_1$ would be needed to effect the same phase shift; greater RF voltage would be applied to the diode under reverse bias. For an arbitrary selection of frequency and diode type, equal loss under forward and reverse bias conditions generally are not achieved coincidentally with maximum power handling capability.

4) *Maximum Power Capability*

a. Continuous maximum RF excitation: Two diode characteristics limit the allowable RF excitation which may be applied to a diode. First, the diode heat dissipation, or thermal resistance, limits either the continuous or average power that may be dissipated in the diode. In the *L*-band model described, each diode dissipates about one-half of one per cent of the incident power. The diode's thermal resistance typically is about 10°C per watt and an additional 10°C per watt might be expected from the circuit mounting. Allowing a maximum temperature rise of 100°C, the diode can dissipate 5 watts continuously and the phase shifter might be operated at continuous RF power levels as high as 1000 watts.

Another limitation in addition to the effects of direct heating has been observed when *p-i-n* diodes are reverse biased. This appears to be related to the amount of RF voltage which is applied to the diode but not particularly related to the pulse duration. With increasing applied RF voltage, it is found that the reverse bias leakage increases after the RF voltage passes a certain threshold. Typically, the average leakage may increase from less than 1 microampere for a reverse bias of −100 volts to an average value of several microamperes, corresponding to a few milliamperes during the RF pulse. Increases of RF applied voltage beyond this level generally precipitate failure of the diode usually as evidenced either by a permanent, short-circuited dc-bias characteristic or a significant decrease in the dc-reverse breakdown voltage.

Arguments for the simplified stress model shown in (Fig. 11) have been advanced [9]. If a high-voltage, several-hundred-volt-breakdown, diode is biased at about −100 volts, a microwave excitation may be applied (shown superimposed on the *V-I* characteristic), which can extend arbitrarily far into the forward region. Little conduction would be expected to occur because the time required to fill the *I* region with charge should be much longer than the half period of the microwave excitation. However, the RF peak excursion is limited in the reverse region by the breakdown voltage; presumably high field breakdown can be precipitated even within the short duration of an RF half cycle. For the particular experimental model described, diodes having reverse breakdown voltages in excess of 900 volts were used, and an applied RF voltage of about 550 volts rms should be sustainable. This corresponds to a peak power level of 43 kilowatts in the 50 ohm circuit described with $22\frac{1}{2}$° phase shift increment per section. Hence, the 1000 watt heat-limited power rating, of course, would apply for continuous operation because it is the lower value.

However, this simplified description of the maximum sustainable RF voltage by the diode describes but one failure mechanism, and others also may prevail. Clearly, the model requires further definition in order to account for nonlinear loss effects. But even in describing the diode's voltage-limited peak power capability, it provides only a coarse estimate. Indeed, the experimental model examined here, as will be seen in the next section, was limited to one third the expected level, although approximation of the circuit model parameters may account for a portion of the discrepancy.

b. Pulsed RF excitation: No higher limits apply regarding average heating and maximum applied voltage to the diode for pulsed operation than were described for continuous operation. An additional limit which usually requires that the average power rating for pulsed operation be less than the continuous rating is encountered, because the diode's heat sinking capacity is very limited. For example, a *p-i-n* switching diode made of a semiconductor die that is 20 mils in diameter and 4 mils high has an estimated heat sinking capacity of about 5 by 10^{-5} joules per degree Centigrade temperature rise.[2] Thus, the experimental phase shifter described would be limited thermally to 0.5 joule of RF pulse energy, assuming a maximum allowable diode temperature rise of 100°C and the same RF losses at high power that were measured at low power.

[2] This heat capacity treatment implies no die cooling during the pulse—a conservatism—and uniform heat dissipation in the die—an optimism; but it is an expedient estimating technique for short pulse cases [7], [10].

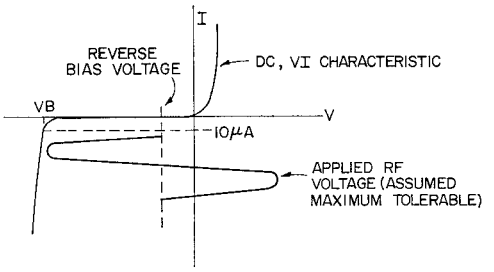

Fig. 11. Diode dc, V-I characteristic with superimposed RF sinusoid.

However, the maximum allowable applied RF voltage serves in this circuit as a primary limiting factor. Measured peak power failure levels are indicated for the various phase shift increments in Fig. 10. Voltage limited peak power handling capability would be expected to increase inversely with the square of the phase shift obtained if other circuit conditions are unchanged. A two diode single section model was constructed and the levels which caused a 10 microampere (indicating incipient breakdown) average reverse bias leakage of each of the diodes were plotted, as shown in Fig. 12. Largest departure from the expected results occurs for the small values of phase shift. However, this was also where the equivalent circuit assumed in Fig. 8 is least accurate, as will be noted in the following subsection. Therefore, it is believed this curve verifies the expected performance within the accuracy of the model.

5) *Phase Shift vs. Frequency Characteristic:* Several factors influence the phase shift vs. frequency characteristic. Four of them which are believed to predominate are listed below, for the practical implementation of the circuit shown in Fig. 8.

1) The difference $\alpha_2 - \alpha_1$ increases with frequency and with it the phase shift.
2) With a change in frequency, the average value $(\alpha_2+\alpha_1)/2$ departs from 90° and then the difference, $B_2 - B_1$, increases due to the cotangent expression, $B_{1,2} = \cot \alpha_{1,2}$.
3) Only approximately does the diode switch between short and open circuits. With forward bias, package inductance and bypass capacity by design are series resonant at the center frequency. At reverse bias, the diode has a capacity, in this case of about 0.8 picofarad.
4) The length and impedance of the spring finger assembly, shorted line behind the diode are known only approximately; largest percentage of error occurs for shortest lengths. (This was where largest departures from calculated performance were measured in the high peak power tests.)

Nonetheless, a fair approximation was achieved even when only 1) and 2) considered with (2) were used to calculate the phase shift variation with frequency. Values calculated thusly are compared with those measured and shown in Fig. 13. The center frequency was redefined to be 1260 Mc/s, that at which the increase of

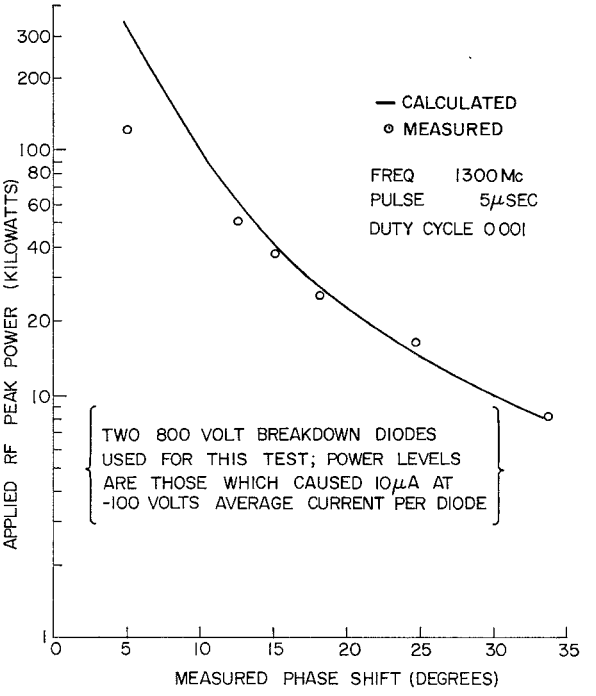

Fig. 12. Measured and calculated phase shift vs. voltage limited peak power capability of L-band model.

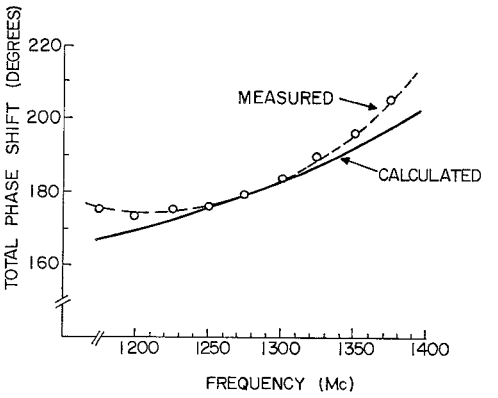

Fig. 13. Measured and calculated phase shift vs. frequency characteristic of L-band model.

phase shift was linearly proportional to the increase in frequency.

B. S-Band Model

1) *Equivalent Circuit:* The *p-i-n* switching diodes already described can be used for a very compact phase shifter implementation at S band. In this frequency range, the inductance and capacitance parameters, often considered parasitic values in switch designs, of the diode and its mount are significant and can be employed to form the switched energy storage elements $jB_{1,2}$ of the desired circuit canonic form. A simplified diode equivalent circuit, shown in Fig. 14(a) was used for the design. The detailed model, shown in Fig. 14(b), was used for evaluation of the measured results. At an operating frequency of 3000 Mc/s, a switchable reactance of $\pm j33$ ohms can be achieved by placing about 1 nanohenry of inductance in series with this diode and

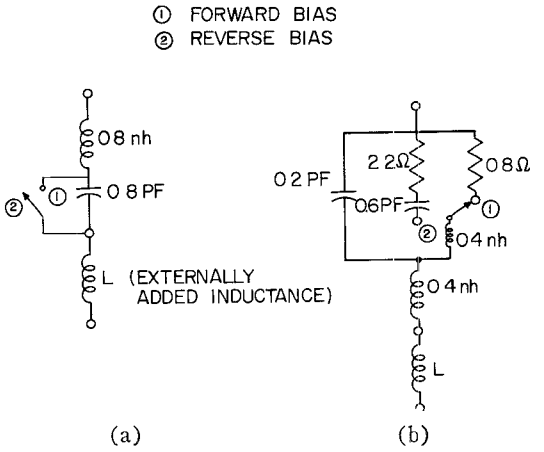

Fig. 14. Diode equivalent circuits used for S-band model. (a) Simplified. (b) Detailed.

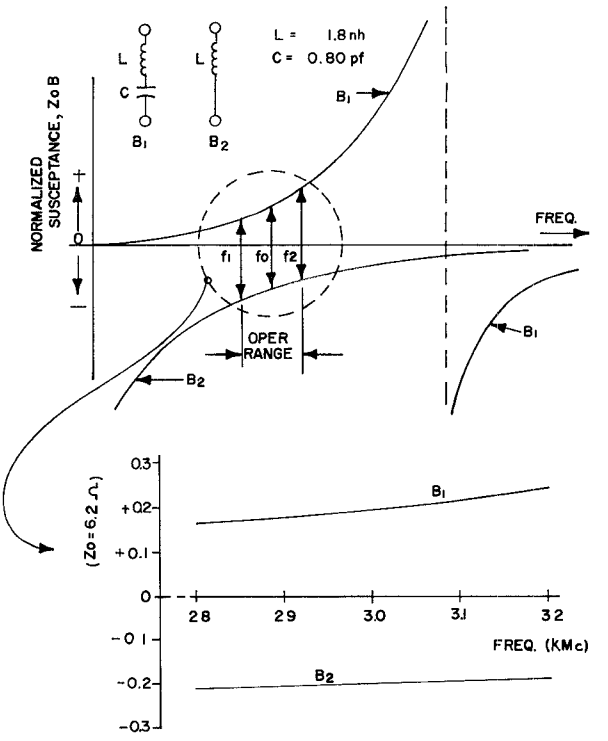

Fig. 15. Switched susceptance vs. frequency characteristic of simplified equivalent circuit used for S-band model.

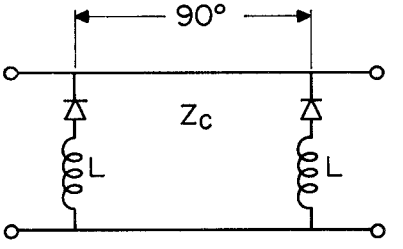

Fig. 16. Equivalent circuit for S-band model prototype section.

almost invariant phase shift with frequency would be expected as indicated by the susceptance plot in Fig. 15.

In turn, a normalized susceptance of $jB_{1,2} = \pm j0.2$ is achieved by mounting the resulting LC combination across a 6.6 ohm characteristic impedance transmission line as shown in Fig. 16.

2) *The Experimental Model:* An eight-section phase shifter model was constructed and is shown pictorially in Fig. 17. Four-section, quarter-wavelength transformers using a Chebyshev reflection coefficient distribution were used to match the desired 50 ohm impedance levels for input and output ports to the low characteristic line impedance in the diode region. The latter was made equal to 6.2 ohms in order to apply tabulated transformer design values [11]. The added series inductance was effected by a small post of adjustable height in series with each diode mount. The post lengths of a single section were adjusted until the measured phase shift of that section was about $22\frac{1}{2}°$ at the design center frequency, 3000 Mc/s; then, all the remaining posts of the 16 diode circuit were made mechanically identical.

The resulting phase shift vs. bias condition is plotted in Fig. 18 along with insertion loss measurements. All were made at low RF power except as noted. The mechanical reproducibility of mounts and approximate similarity of diodes used produced very nearly the same phase shift for all of the sections. The incremental transmission phase perturbations effected by successively reverse biasing diode pairs varied from 20° to 23° at 3000 Mc/s.

The maximum input VSWR and insertion loss of the circuit with diodes removed were 1.25 and 0.3 dB, respectively, over the 2800 to 3200 Mc/s frequency range. The maximum, low RF power level, insertion loss with diodes installed in the circuit occurred when all were forward biased and was 0.9 dB. Using the mean values for the detailed equivalent circuit reactance parameters of Fig. 14(b), the value for L consistent with $22\frac{1}{2}°$ of phase shift per section is calculated to be 0.5, rather than 1, nanohenry. Taking circuit losses into account, the loss per forward biased diode was 0.037 dB and corresponds to a value of $R_F = 0.8$ ohm; similarly the value for R_R implied is 2.2 ohms. These values include the loss effects of the mountings, which may account for the somewhat high values. Also, the diodes actually may differ from those whose measurements were reported and presumed typical. Loss equalization could be obtained by increasing the series inductance L. The corresponding diminution of phase shift could be compensated by increasing the transmission line impedance; however, both changes would decrease the RF voltage limited peak power capability.

The measured phase shift variation with frequency is shown and was very nearly the same, +4 per cent, for a 200 Mc/s increase or decrease in RF frequency. The calculated change, using (2), is 1 per cent or less over this frequency interval.

3) *Maximum Power Capability:* Using the detailed circuit model of Fig. 14(b), with $L = 0.5$ nanohenry, it can be seen that at reverse bias the RF voltage across

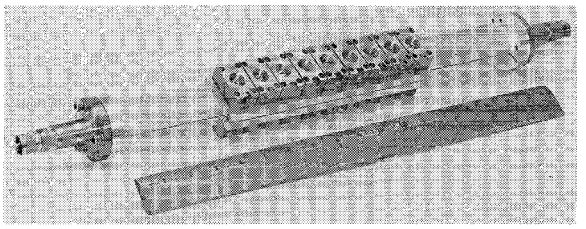

Fig. 17. Photograph of eight-section (16 diode) *S*-band transmission phase shifter model.

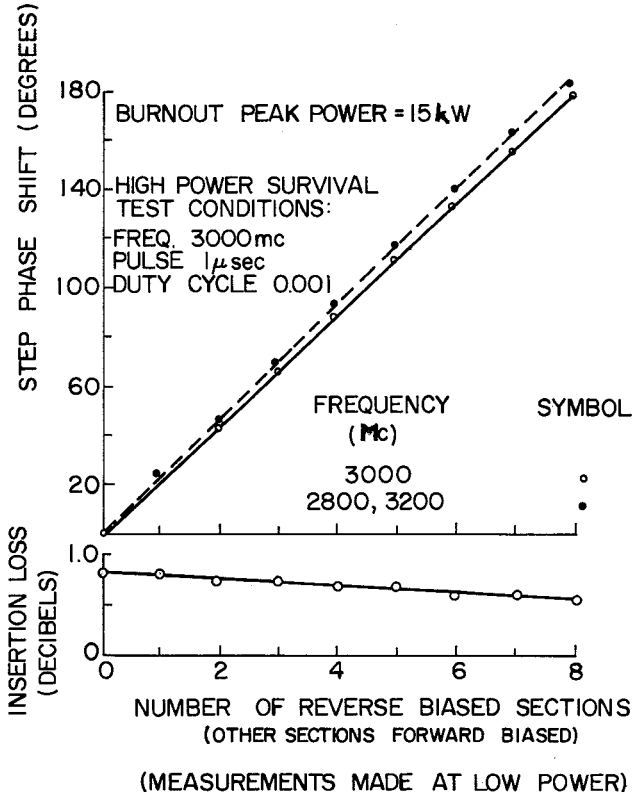

Fig. 18. *S*-band measurements of phase shift, insertion loss and ultimate peak power capability.

the junction capacity C_j is about 1.6 times that delivered to a matched load terminating the 6.2 ohm line. Using the voltage limited peak power argument advanced previously and the same 900 volt breakdown diodes, a peak input power capability of 16 kilowatts at 3000 Mc/s is calculated. Interestingly, the model was so tested and first diode failures did occur at 15 kilowatts. A useful short-pulse-length operating level for such a phase shifter might be in the (5 to 10) kilowatt peak power range. Since the maximum insertion loss per diode was about 0.04 dB, continuous RF power levels up to 500 watts should be sustainable.

A similar phase shifter, having only two sections was constructed in still a lower transmission line impedance, 3.3 ohms. The diodes and mountings were unchanged. The model yielded only about 11° of phase shift per section and was tested to a burnout level of 37 kilowatts under the same conditions. Insertion loss was 0.3 dB and was principally attributable to circuit losses.

IV. Conclusions and General Comments

The transmission phase shifter using *p-i-n* diode control elements is quite amenable to *L*- and *S*-band implementation. It forms a straight path, compact cross section circuit suited to dense positioning in a phase steerable array antenna. The distributed nature of the circuit enhances sharing by the diodes of the phase shift-power stresses. Burnout peak power levels of 15 kilowatts were reached with $\frac{1}{16}$th wavelength phase shift and (0.06 to 0.10) decibel average insertion loss per section in the *L* and *S* frequency bands, respectively. Higher peak power operation to 140 kilowatts at *L* band was sustained with reduced phase shift per diode. Useful operating bandwidths of 20 per cent should be obtainable under most performance requirements.

Considerable flexibility exists in the implementation. If up to 45° phase shift per section is taken, which probably is possible without severe mismatch effects, and if line loading element pairs at common points are designed to use just one diode a 360° 4-bit transmission phase shifter could be designed to use only 12 diodes. Some degradation of insertion loss, peak power, and bandwidth performance likely would be required, however.

The approach described should be extendible for frequency ranges above and below those described. The reproducible nature of this circuit together with the advantages of semiconductor control with *p-i-n* diodes suggest this approach will prove useful for array antenna beam steering.

Acknowledgments

The author wishes to thank the many persons who contributed to the study, especially K. E. Mortenson, M. E. Hines, L. Mesler, L. J. Ricardi, H. Griffin, G. Garas, H. Esterly, and E. M. Chinn.

References

[1] Mortenson, K. E., Microwave semiconductor control devices, *Microwave J.*, May 1964, pp 49–57.
[2] White, J. F., Semiconductor microwave phase control, *NEREM Digest*, Nov 1963, pp 106–107.
[3] Allen, J. L., D. H. Temme, et al., Phased array radar studies, Tech Rept No 299, MIT Lincoln Lab., Lexington, Mass., Jul 1961–Jan 1963.
[4] Stark, L., R. Burns, et al., Interim development report for phased array study (unclassified) sponsored by Contract NObsr-89427, Hughes Aircraft Co.
[5] Hines, M. E., Fundamental limitations in RF switching and phase shifting using semiconductor diodes, *Proc. IEEE*, Jun 1964, pp. 697–708.
[6] Simmons, A. J., Phase shift by periodic loading of waveguide and its application to broad-band circular polarization, *IRE Trans. on Microwave Theory and Techniques*, vol MTT-3, Dec 1955, pp 18–21.
[7] Leenov, D., The silicon *pin* diode as a microwave radar protector at megawatt levels, *IEEE Trans. on Electron Devices*, vol ED-11, Feb 1964, pp 53–61.
[8] DeLoach, B. C., A new microwave measurement technique to characterize diodes and an 800 Gc cutoff frequency varactor at zero volts bias, *IEEE Trans. on Microwave Theory and Techniques*, vol. MTT-12, Jan 1964, pp 15–20.
[9] Mortenson, K. E., private communication.
[10] Hines, M. E., private communication.
[11] Young, L., Tables for cascaded homogeneous quarter-wave transformers, *IRE Trans. on Microwave Theory and Techniques*, vol MTT-7, Apr 1964, pp 233–237.